Manuscript

Shaposhnikov Dmitry Sergeevich

NUMERICAL SIMULATION OF THE HYDROLOGICAL CYCLE OF MARS

Specialty 01.03.04 — «Planetary Research»

Synopsis

Moscow — 2019

The work has been performed at the Department of Space Physics of the Moscow Institute of Physics and Technology in the Space Research Institute of the Russian Academy of Sciences.

Scientific supervisor:	Candidate of Physical and Mathematical Sciences, Associate Professor **Rodin Alexander Vyacheslavovich**
Lead organization:	A.M. Obukhov Institute of Atmospheric Physics Russian Academy of Sciences

The defense will take place 18.12.2019 at 10:00 at the meeting of the dissertation council ЛФИ.01.03.04.001 of the Moscow Institute of Physics and Technology by the address:
9 Institutskiy per., Dolgoprudny, Moscow Region, 141700, Russian Federation.

The dissertation can be found in the library and on the website of the Moscow Institute of Physics and Technology:
https://mipt.ru/education/post-graduate/soiskateli-fiziko-matematicheskie-nauki.php

Feedback on the author's synopsis in two copies, certified by the seal of the institution, please send to: 9 Institutskiy per., Dolgoprudny, Moscow Region, 141700, Russian Federation, scientific secretary of the dissertation council ЛФИ.01.03.04.001.

The work was submitted 09.10.2019 to the Attestation Commission of the Moscow Institute of Physics and Technology for consideration by the council for the defense of dissertations for the degree of candidate of science, doctor of science in accordance with paragraph 3.1 Art. 4 of the Federal Law «On Science and State scientific and technical policy».

На правах рукописи

Шапошников Дмитрий Сергеевич

ЧИСЛЕННОЕ МОДЕЛИРОВАНИЕ ГИДРОЛОГИЧЕСКОГО ЦИКЛА МАРСА

Специальность 01.03.04 — «Планетные исследования»

Автореферат

Москва — 2019

Работа выполнена на кафедре космической физики Федерального государственного автономного образовательного учреждения высшего образования «Московский физико-технический институт (национальный исследовательский университет)» в Федеральном государственном бюджетном учреждении науки Институт космических исследований Российской академии наук.

Научный руководитель:	кандидат физико-математических наук, доцент **Родин Александр Вячеславович**
Ведущая организация:	Федеральное государственное бюджетное учреждение науки Институт физики атмосферы им. А.М. Обухова Российской академии наук

Защита состоится 18.12.2019 в 10:00 на заседании диссертационного совета ЛФИ.01.03.04.001 Федерального государственного автономного образовательного учреждения высшего образования «Московский физико-технический институт (национальный исследовательский университет)» по адресу: 141700, Россия, Московская область, Институтский пер., 9.

С диссертацией можно ознакомиться в библиотеке и на сайте Московского физико-технического института (национального исследовательского университета):
https://mipt.ru/education/post-graduate/soiskateli-fiziko-matematicheskie-nauki.php

Отзыв на автореферат в двух экземплярах, заверенный печатью учреждения, отправлять по адресу: 141700, Россия, Московская область, Институтский пер., 9, ученому секретарю диссертационного совета ЛФИ.01.03.04.001.

Работа представлена 09.10.2019 в Аттестационную комиссию Федерального государственного автономного образовательного учреждения высшего образования «Московский физико-технический институт (национальный исследовательский университет)» для рассмотрения советом по защите диссертаций на соискание ученой степени кандидата наук, доктора наук в соответствии с п. 3.1 ст. 4 Федерального закона «О науке и государственной научно-технической политике».

General description of work

Research relevance and Literature review

Studying the planets and small bodies of the Solar System is of paramount importance for understanding its origin and development. But above all, it provides the key to finding the likely paths of the future evolution of our planet and understanding how to keep Earth habitable for future generations.

Mars is the fourth planet from the Sun in the Solar System and the closest one to Earth among the other planets. At present, Mars is the most interesting and the most explored planet of the Solar System after Earth. The climate conditions on Mars, although being unsuitable for life, are the most similar to those on Earth. Presumably, in the past, the Martian climate could have been warmer and wetter; there was liquid water on its surface, and it even rained. Mars is the most likely destination for the first manned mission to another planet. However, the main thing is that Mars is so far the only planet that holds promise in terms of human development.

The Martian climate is mainly determined by the processes occurring in its atmosphere, such as the movement of air masses, convective mixing, radiative transfer, and transport of tracers. It is impossible to measure atmospheric fields, e.g. velocity, in full detail, neither on Earth, nor on other planets. Therefore, the unknown parameters can be derived from those obtained in experiments by building numerical climate models of general or global atmospheric circulation (GCMs). The majority of the well known models are based on numerical solution of the 3D equations of geophysical fluid dynamics (GFD).

One of the first attempts to numerically describe the atmosphere of Mars was made by Leovy and Mintz (1969), who successfully adapted the GCM developed at the University of California (Los Angeles) to the Martian conditions. Since then, Martian GCMs proliferated. To date, there are several models of sufficient complexity, which were developed in the United States, France, Britain, Japan, Canada, and Germany. They are used for investigation of a wide range of processes and phenomena in the Martian atmosphere and for interpretation of observational data. The availability of plentiful measurements of water vapor stimulated attempts to simulate the water cycle with the Martian GCMs.

Water in its different phases is a very important element of the current Martian climate, being a sensitive marker of meteorology in the atmosphere. It affects the Martian climate mostly through radiative effects of water ice clouds and scavenging dust from the atmosphere. Water was first detected in the Martian atmosphere more than a half century ago. The next generation of studies broadly utilized data from orbiting and landing spacecraft, e.g., from Mars Atmospheric Water Detector (MAWD) onboard the Viking Orbiter. To date, the main sources of information about the water distribution in the Martian atmosphere are the Thermal Emission Spectrometer (TES) onboard Mars Global Surveyor (MGS), the Mars Climate Sounder (MCS) and the Compact Reconnaissance Imaging Spectrometer for Mars (CRISM) onboard Mars Reconnaissance Orbiter (MRO), the LIDAR instrument onboard the Phoenix Lander and the Planetary Fourier Spectrometer (PFS), the Visible and Infrared Mineralogical Mapping Spectrometer (OMEGA), the Spectroscopy for Investigation of Characteristics of the Atmosphere of Mars (SPICAM) instruments onboard Mars Express and the Atmospheric Chemistry Suite (ACS) and Nadir and Occultation for Mars Discovery (NOMAD) instruments onboard ExoMars Trace Gas Orbiter (TGO).

The history of the water cycle modeling starts from the work of Davies (1981) who has developed a model to test the hypothesis that the observed seasonal and latitudinal distribution of water on Mars is controlled by sublimation and condensation of surface ice deposits in the polar regions, and by the meridional transport of water vapor. Then, James (1990) used a 1D model to show the role of water ice clouds in the water migration from north to south. The first comprehensive microphysical model of clouds was developed by Michelangeli et al. (1993) following the earlier attempts undertaken after measurements of water vapor vertical profiles. Colaprete et al. (1999) used microphysical models and Haberle et al. (1999) employed a Martian general circulation model (MGCM) to reproduce observations provided by Mars Pathfinder. Richardson and Wilson (2002) and Richardson et al. (2002) used the Geophysical Fluid Dynamics Laboratory (GFDL) MGCM to simulate the annual water cycle on Mars and compared it with the Viking MAWD data. Although the simulated climate was overly wet, these studies revealed the key mechanisms of the water transport. A more sophisticated model, which included transport, phase transitions and microphysical processes, has been developed by Montmessin et al. (2004). Later a microphysical model for Mars dust and ice clouds has been applied in combination with a model of the planetary boundary layer (PBL) for interpretation of measurements by the LIDAR instrument on the Phoenix Mars lander. Observations of temperature inversions in the atmosphere of Mars have motivated modelers to include effects of radiatively active water ice clouds (RAC) in MGCMs. These studies have demonstrated that accounting for RAC helped to reduce global temperature biases between simulations and observations at northern spring and summer. More MGCMs that include water cycle have been developed to date: DRAMATIC (Dynamics, RAdiation, MAterial Transport and their mutual InteraCtions) MGCM, NASA Ames GCM, GEM-Mars (The Global Environmental Multiscale model for Mars) GCM, the Laboratoire de Météorologie Dynamique (LMD) MGCM and the Oxford University MGCM. The cloud scheme described by Montmessin et al. (2004) was implemented at least in the latter two models, while the Oxford MGCM also used data assimilation scheme to nudge the simulated temperature to available observations.

In order to successfully reproduce water cloud formations in the atmosphere of Mars, microphysical models require a correct prediction of the size distribution of aerosol particles, which serve as cloud condensation nuclei (CCN). Several observations have provided the evidence that this distribution is bimodal. The distribution is called bimodal if its density function has two peaks, or modes. Montmessin et al. (2002) implemented such distribution into their one-dimensional model, prescribing two peaks with constant effective radii and variance for fine and large modes with a fixed ratio between them. They indicated that this assumption improved the simulations. For instance, it resulted in decrease of the effective radii of ice particles condensing on the CCN. In the second chapter of this study, we focus on the effects of the bimodal dust distribution on the global hydrological cycle.

As it was stated, water is a minor component of the Martian atmosphere, which is largely confined within a few lower scale heights. Nevertheless, it is also the main source of hydrogen in the upper atmosphere. Escape of hydrogen atoms into space near the exobase varies by an order of magnitude seasonally, maximizing around southern summer solstice (solar longitude $L_s \approx 270°$), according to MAVEN and HST observations during dust storms. Observed water in the lower atmosphere also experiences strong seasonal changes and depends on airborne dust load. This implies a link between water in the troposphere and thermosphere and a corresponding mechanism of transport between the layers.

The Martian middle atmosphere is too cold to sustain water vapor in large amounts, especially around the mesopause, while ice particles are sufficiently heavy and prone to sedimentation. This water behavior is similar to that in the terrestrial middle atmosphere. However, there are multiple observations showing a presence of water vapor in the middle atmosphere at certain locations and times. Heavens et al. (2018) and Fedorova et al. (2018) provided evidence of strong seasonal variations of the globally averaged water abundance and its vertical extension up to 70-80 km at perihelion during the Martian Year 28 (MY28) global dust storm. Hypotheses concerning the mechanism of vertical transport of water include mesoscale deep convection, turbulent mixing in the lower atmosphere and/or an unspecified dynamics in the upper atmosphere. General circulation modeling underestimates the hygropause altitude at southern summer solstice to date. The third chapter of this study addresses this gap in knowledge of processes that couple water in the lower and upper atmosphere.

The **aims** of the present research are *to conduct numerical simulations of the Martian hydrological cycle using a state-of-the-art MGCM and investigate 1) the influence of various factors, including the bimodality of dust distribution, on water vapor and ice and 2) the mechanism of water exchange between the lower and upper atmosphere.*

To achieve the mentioned goals, it is necessary to solve the following **research objectives**:

1. Develop a numerical hydrological scheme and implement it in an existing MGCM dynamical core. The comprehensive scheme has to account for advective transport, mixing by diffusion, particle size distribution, sedimentation, spatio-temporal variations of atmospheric dust, water saturation, sublimation, nucleation, ice particle growth and water photodissociation.
2. Simulate the hydrological cycle during several Martian years.
3. Investigate the effects of the bimodal dust size distribution on water cycle.
4. Explain the mechanism of water exchange between the lower and upper atmosphere.
5. Compare the results with existing observational data from orbiters and landers.

The hydrological scheme used in the study is based on the approach from the works of Montmessin et al. (2002, 2004) and Navarro et al. (2014). It is implemented into the Max Planck Institute (MPI) MGCM (also known as MAOAM – Martian Atmosphere Observation and Modeling). This model with the employed physical parameterizations have been described in detail in the works of Hartogh et al. (2005, 2007) and Medvedev and Hartogh (2007). The most recent applications of this MGCM along with the current setup are presented in the works of Medvedev et al. (2013, 2015, 2016) and Yiğit et al. (2015).

Scientific Novelty

There is a number of innovations implemented into the hydrological scheme, which have allowed to obtain absolutely new scientific results.

1. A new accurate bimodal dust parameterization based on the SPICAM observational data has been used. Since, dust plays a key role in the Martian hydrological cycle in the low and middle atmosphere, its precise parameterization is critically important for simulations of water.

2. Simulations with the bimodal dust distribution have been performed with the 3D model for the first time. Previous studies used only one-dimensional models and, thus, could not reproduce the water cycle in detail.

3. The model domain has been extended into the thermosphere up to ∼160 km. It is one of the two existing MGCMs covering the atmosphere from the ground to almost the exobase, and the only one that employs accurate parametrization of gravity waves in the middle and upper atmosphere. Coupled with the sophisticated hydrological scheme, the MGCM represents a state-of-the-art extended model.

4. The water photodissociation scheme has been implemented in the model to account for the major mechanism of water supersaturation suppression in the upper atmosphere.

5. Systematic errors of commonly used nucleation and particle growth schemes have been discovered and explored. A way of reducing these errors has been proposed.

To sum up, this is the first modeling study that considers in greatest detail the transport of water from the surface to the thermosphere of Mars and explores its links with the atmospheric dust cycle.

Theoretical and Practical value of the study

The results of hydrological cycle simulations can be used for current and future Mars missions in, at least, three different ways. First, the model produces surface map of ground water ice with the prescribed resolution (5.625° in the current work). It could help in selection of landing sites for landers focusing on ground water ice research. The choice of the landing place under such conditions plays an important role in the success of the missions. Second, the predicted by the model wind, temperature and density can help to optimize the landing operations. Of course, the climate model cannot forecast weather at specific time and point, but it can predict main atmospheric features and their variations. Third, simulated vertical distributions of atmospheric tracers such as water vapor and ice can be used for assisting remote sensing performed from orbiters. Other future applications of the model, like forced climate change, climate evolution, or Martian terraforming, require significant modifications of the scheme, but also could be considered.

Theoretical aspects of the model applications include cross-validations with other GCMs, exploring paleoclimate and evolution, testing climate hypotheses, equations and assumptions used in simulations.

Methodology and research methods

The MPI-MGCM employs a spectral dynamical core to solve the primitive equations of geophysical fluid dynamics on a sphere. The physics and tendencies are calculated on a 3D grid, and then are transformed into spectral coefficients at every time step. In the vertical, the grid is defined in the hybrid

η-coordinate discretized into levels, terrain-following near the surface and pressure based near the top. The horizontal grid is based on the Gauss-Kruger map projection with 32 and 64 bins in latitude and longitude, respectively. This discretization corresponds to a T21 triangular spectral truncation, which is a typical resolution of currently employed MGCMs, with a few exceptions for high-resolution experiments. Finite spatial resolution can be a source of numerically-induced features in simulations, which is discussed in the text.

The spectral dynamical core is not well suited for simulation of the tracer transport. Instead, the advection scheme based on a semi-Lagrangian explicit monotonous second-order hybrid scheme and the time splitting method in three spatial directions are adopted. A thorough examination of performed runs has confirmed that this scheme maintains a high order of conservation of water masses and solution accuracy appropriate for general circulation modeling. In addition to advection, transport includes diffusion and mixing associated with subgrid-scale processes. The importance of vertical eddy mixing for modeling the water cycle was emphasized by Richardson and Wilson (2002). In our simulations, the Crank-Nicolson implicit method with the Richardson number-based diffusion coefficients is used to solve the vertical diffusion equation.

The results of simulations have been validated with observational data obtained from TES, SPICAM, CRISM, MCS and other instruments.

Statements to be defended:

1. A new microphysical scheme for water cycle on Mars implemented in a 3D general circulation model.
2. Accounting for bi-modality of aerosol particle size distribution improves simulations of water ice characteristics in the model compared to observations.
3. The fine fraction of atmospheric aerosols weakly affects spatial distribution of water vapor in the model.

4. Global circulation modeling reveals the mechanism of water exchange between the lower and upper atmosphere.
5. Atmospheric dust controls the circulation strength and, hence, the amount of high-altitude water.
6. Solar tide modulates the upwelling of water vapor by almost completely shutting it down during certain local times.

Presentation and validation of research results

The reliability of the simulation results is confirmed by comparison with known observational data and the results of other models. The main results of the work were reported at 18 conferences, 9 of which are international, e.g.:

1. International Forum «SpaceKazan–IAPS–2015», Kazan, Russia, 2015;
2. II International Scientific Conference «Science of the Future», Kazan, Russia, 2016;
3. International Scientific Conference «AGU Fall Meeting 2016», San Francisco, United States, 2016;
4. «The Sixth International Workshop on the Mars Atmosphere: Modeling and Observations», Granada, Spain, 2017;
5. International «Les Houches winter school on the planetary atmospheres», Les Houches, France, 2017;
6. International Workshop «6th ACS science working team», Suzdal, Russia, 2018;
7. International Scientific Conference «Asia Oceania Geosciences Society Annual meeting», Hawaii, USA, 2018;
8. The First International Aerospace Symposium «The Silk Road», Moscow, Russia, 2018;
9. International Scientific Conference «AGU Fall Meeting», Washington, USA, 2018.

Publications

The main results of the thesis are presented in 6 publications [1—6], 3 of which are published in refereed journals included in Web of Science and Scopus and recommended by Higher Attestation Commission [1—3], 3 — in conference proceedings [4—6]. The certificate of state registration of computer program №2019611779 was obtained by the author [7].

Personal Contribution

The program code of the hydrological scheme and aerosol microphysics had been developed and implemented by the author. All numerical experiments had been carried out and processed by him. The author was the first author of all his publications and the correspondence with editorial offices and referees has been run by him as well. The content of the articles had been written by the author in cooperation with the co-authors.

Volume and structure of the work

The thesis consists of an introduction, four chapters, a summary and conclusions. The full volume of the thesis is **102** pages, including **26** figures and **3** tables. The bibliography contains **135** cites.

This study has been performed at the Laboratory of Applied Infrared Spectroscopy of Moscow Institute of Physics and Technology in cooperation with Max Planck Institute for Solar System Research. The work was partially supported by the Russian Science Foundation Grant 16-12-10559 and German Science Foundation (DFG) Grant HA3261/8-1.

The content of the work

The introduction justifies the relevance of the research conducted within the framework of this thesis, provides an overview of the scientific literature on the problem under study, formulates an aim and sets research objectives of the work, the scientific novelty and theoretical and practical value of the presented work. In subsequent chapters, the general principle of the model is described first, followed by a description of the hydrological scheme, numerical experiments conducted, a comparison with observational data and conclusions.

The first chapter briefly describes the general characteristics of the planet Mars. **The first section of the chapter** reveals the orbital and physical parameters and the surface topography of the planet. Mars is the forth planet from the Sun, closest outer planet to Earth. It has an eccentricity similar to Earth, as a result of which there is a change of seasons on Mars.

The second section of the chapter reveals the composition of the Martian atmosphere. The atmosphere mainly consists of carbon dioxide. Water vapor is only 0.03% of the atmosphere. The average surface pressure is about 600 Pa. The temperatures of the atmosphere and surface vary widely from ~ 145 K (carbon dioxide condensation temperature) to ~ 300 K. The orbit of Mars has a quasi-chaotic nature. It occurs mainly due to the influence of Jupiter tides and to the absence of a large moon which can act as stabilizer. The obliquity of the Mars varies from $\sim 15°$ to $\sim 45°$ during the last 10 million years, which can affect the hydrological cycle as well.

The third sections of the chapter reveals the water physics under the Martian conditions. In the atmosphere of the Earth water can be in three physical states: gaseous (vapor), liquid, and solid (ice). On the contrary, under the Martian conditions only two states stable occur – vapor and ice.

The forth section of the chapter describes the present hydrological cycle of Mars and the past investigations. The water content in the northern hemisphere is almost an order of magnitude higher than in the southern one. Historically there were several points of view on this problem. According to modern concepts the most important thing in the water cycle of Mars is the exchange between the northern polar cap, which is the main reservoir of water on the planet, and the atmosphere that controls spring / summer evaporation and winter / autumn return (condensation) of water to the pole.

The second chapter is devoted to the description of the MGCM and the hydrological cycle scheme. A detailed description of the employed basic equations is given, the limits of applicability of the methods are established, and the formulation of the problem is explained in terms of the numerical scheme.

The MPI-MGCM model used in the research is based on the spectral dynamical core of COMMA/IAP (Cologne Model of the Middle Atmosphere / Institute of Atmospheric Physics, Kühlungsborn, Germany), a terrestrial GCM which was extensively used for studies of the dynamics and photochemistry of the middle atmosphere. The Earth models themselves could not be directly used to simulate the Martian atmosphere, because the latter is much thinner, wind velocities are greater, and variations of the field variables are stronger. These all lead to instability of the model, therefore, a specific modification of the numerical core is required. The MPI-MGCM model implements many changes in the COMMA/IAP, e.g. a new time stepping scheme, vertical discretization, and the horizontal diffusion parameterization. Also, it contains a comprehensive set of physical parameterizations relevant to the altitude range from the surface up to 160 km. MPI-MGCM was thoroughly validated with observations and through intercomparisons with other models. It successfully reproduces the atmospheric structure and circulation and was applied to studying various processes in the Martian atmosphere, including a novel CO_2 15 mm band radiation scheme for the non-LTE (local thermodynamic equilibrium).

The first section of the chapter describes the governing equations of the MPI-MGCM. All the equations are transformed to the terrain-following vertical hybrid coordinates η. *The vertical domain* of the model is divided into 50 pressure levels for the basic version (up to 110 km) and 67 levels for the extended one (up to 160 km). Pressure p is represented as a function of η and surface pressure p_s:

$$p(\eta; p_s) = a(\eta) + b(\eta)p_s. \tag{1}$$

The coefficients a and b guarantee monotonous growth of p with η, as well as the boundary conditions $p(\eta = 0; p_s) = 0$ and $p(\eta = 1; p_s) = p_s$. The flexibility of (1) is used to let surfaces of constant η correspond to terrestrial σ-levels near the ground and to pressure levels at high altitudes. This parameterization allows one to track the unevenness of the surface relief and reduce the movement of impurities between the cells in the vertical direction.

The prognostic differential equations for horizontal divergence D, vorticity ξ, temperature T, and surface pressure p_s are represented following Simmons and Burridge (1981).

Then, having fixed intermediate hybrid n_{lev} levels, it is possible to restore the intermediate (interface) pressure levels using (1). Full pressure levels and centered pressure differences are defined as a sum and difference of intermediate levels, respectively. This finite-difference representation in the vertical provides energy and angular momentum conservation properties following Simmons and Burridge (1981).

The horizontal grid is based on the Gauss-Kruger map projection with 32 and 64 bins in latitude and longitude, respectively. This corresponds to the so-called T21 truncation of *spherical harmonics* $Y_{n,m}$. All the prognostic and diagnostic equations are expanded in series of these spherical harmonics. In particular, the notation T21 indicates that all the fields are represented by 21 harmonics in the zonal direction. This approach allows to separate time tendencies and numerical time increments by application of Galerkin's method at each full model layer.

Thus, for each spectral mode n, m (except $n = 0$) the tendency vector $T_{n,m}$ could be written as a matrix decomposition:

$$\mathbf{T}_{n,m} = \mathrm{A}_n \mathbf{y}_{n,m} + \mathbf{T}'_{n,m}. \tag{2}$$

Here $\mathbf{T}'_{n,m}$ represents all model tendencies like Coriolis force, nonlinearities, diffusion, gravity wave forcing, and diabatic heating. The matrix A_n describes the buoyancy oscillations of a horizontally uniform reference state, e.g. the internal gravity waves in a corresponding linearized model version without any other physical parameterizations. The vector $\mathbf{y}_{n,m}$ represents the unknown variables.

The equation (2) can be then rewritten to obtain required $\mathbf{y}_{n,m}$ and its numerical representation using inverse matrices. In order to numerically integrate the obtained system, the semi-implicit leapfrog scheme is used. The scheme must be completed by a time filter to damp the numerical instabilities.

The second section of the chapter describes the hydrological scheme implemented in the model. The spectral dynamical core is not well suited for simulation of the *tracer transport*. Instead, the advection is calculated using the semi-Lagrangian explicit monotonous second-order hybrid scheme and the time splitting method in three spatial directions. The scheme has substantial advantages due to its higher order of conservation, stability and retaining sharp gradients of transported quantities. These all are very important for modeling atmospheric parameters like water vapor and ice.

The second group of processes affecting traces are *turbulent and molecular diffusions*. The importance of vertical turbulent diffusion or eddy mixing for modeling the water cycle was emphasized by Richardson and Wilson (2002). The best agreement with the experimental data in the basic model version (50 levels) is obtained using a simple Crank-Nicolson implicit method with the constant coefficient equal to 10 $m^2 s^{-1}$ for vertical diffusion. In the extended version of the model, the diffusion coefficients were not fixed, but had been computed by the dynamical core of the model. This required a specific adaptation of the diffusion scheme in order to preserve the conservation properties of the scheme on sharp gradients of the diffusion coefficient in neighboring cells.

The implemented hydrological scheme includes the transport of water vapor and ice particles, the sizes of which are subdivided into *bins*. Each bin has its own size of dust condensation nuclei. 4 bins with average radii 0.1, 0.5, 1, 5 μm are used. A two-moment scheme is used for every bin while maintaining separately the ice mass and number of particles.

In the model for water ice particles, the *sedimentation* is calculated using the Stokes formula with the Cunningham correction. As already mentioned, the vertical cells represent the different pressure levels. Then, the derivative $\mathrm{d}p/\mathrm{d}t$ acts as a vertical velocity in pressure coordinates. It is now possible to calculate the sedimentation correction to particle's velocity using the equation:

$$\frac{\mathrm{d}p}{\mathrm{d}t} = \frac{2}{9}\rho_i g^2 \frac{R_i^2}{\nu}\Big(1 + A_+ \frac{\lambda}{R_i}\Big), \tag{3}$$

where A_+ is the Cunningham correction, ρ_i is the ice density, g is the acceleration of gravity, R_i is the radius of ice particles (consider them to be spherical), ν is the kinematic viscosity, and λ is the average length of the free path in the gas depending on pressure.

One of the most important novelties of the model is *the bimodal dust distribution*. It employs a predetermined dust scenario that represents a seasonal evolution of the zonally averaged aerosol optical depth τ in the thermal IR based on the MGS-TES and MEX-PFS measurements with the global dust storms removed (the so-called “MGCM dust scenario”). Thus, dust is not transported in the model. The CCN number density in each bin can be calculated from, for instance, the bimodal log-normal dust distribution, as shown in Figure 1.

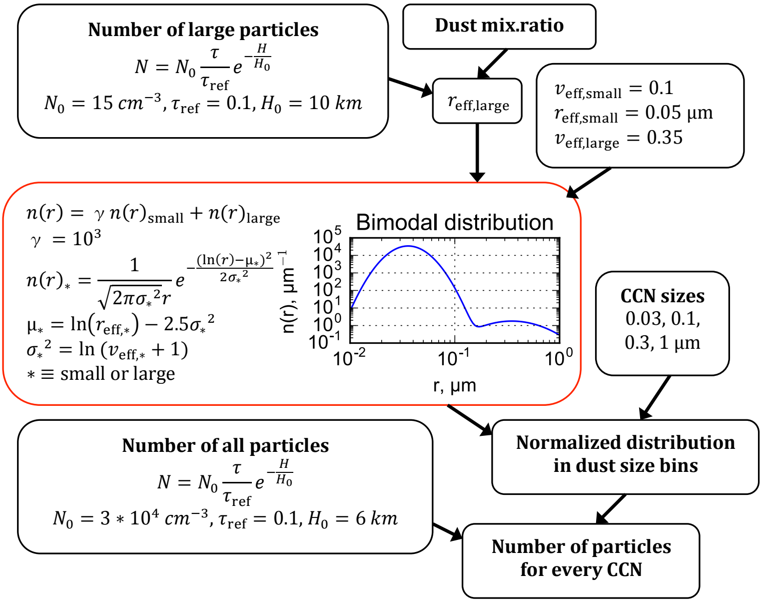

Fig. 1 — The operation scheme for calculating the bimodal dust distribution. N is the number density of large/small particles, τ is the dust optical depth in a vertical column (“MGCM dust scenario”), H is the altitude of the grid cell, $r_{\rm eff}$ is the effective radius, $v_{\rm eff}$ is the effective variance, γ is the population ratio, $n(r)$ and $n(r)_*$ are the bimodal and mono-modal size distribution functions, correspondingly.

It is need to consider water microphysics next. The water vapor *saturation* in a grid cell determines the amount of vapor that the cell holds. The water vapor saturation pressure on Mars as a function of temperature is expressed through a modification of the August-Roche-Magnus formula.

Water ice clouds are formed when water vapor nucleates on dust particles, on the so-called *cloud condensation nuclei* (CCN). In the earlier version of the model [1], the cloud scheme was rather simple: water vapor is turned instantaneously into ice (or vice versa) reaching the saturation pressure, the number of ice particles was ignored. The later versions of the model [2; 3] use a two-moment scheme with 4 bins for different mean nuclei core sizes. For water ice condensing on dust nuclei, a heterogeneous nucleation rate is required. For this, the homogeneous (without the aid of a pre-existing surfaces) homomolecular (nucleation of high molecular weight) nucleation rate is obtained first, and then related it to its heterogeneous counterpart. The number of active CCN also depends on a parameter $m_h = \cos\theta$, where θ is the "contact angle" (for the liquid phase, it is the angle of the interface between the droplet and its nucleus). $m_h = 0.95$ is used in the basic and $m_h = 0.96$ in the extended model versions, which is consistent with the typical range for Martian dust between 0.93 and 0.97. There are indications that the value of this parameter significantly affects the simulated distributions of water.

Once the ice has condensed, the particles are prone to growth based on various factors. The *rate of growth* is a function of the water vapor saturation ratio, saturation pressure ratio over a curved surface, molecular diffusion resistance and the heat release.

The water cycle is fed by the water sublimating from the surface. The mechanism that maintains the *sublimation* is based on the turbulent flux of water at the bottom of the atmosphere.

The last point used only in the extended model is the water vapor *photodissociation*. Unlike with earlier simulations of the water cycle [1; 2], the latter model covers the domain extending into the thermosphere, where water is no longer chemically conservative, and an accurate photochemical modeling may have to be included depending on the motive. For purposes of this work, only a parameterization of H_2O losses due to photodissociation have been retained. The water photodissociation rates have been calculated according to Anbar et al. (1993).

The third chapter discusses the influence of the bimodal dust distribution on the simulated hydrological cycle. **The first section of the chapter** describes the design of simulations. The model runs have been initialized with the distribution of water vapor in the atmosphere obtained in the earlier experiments [1]. The previous simulations started with a linear latitudinal gradient of water vapor (from 0 in the south to 200 ppm in the north), and no ice outside of the caps was prescribed anywhere in the atmosphere at the beginning. Then, spin-up runs have been performed for several Martian years. The results to be presented in the chapter are based on daily averaged quantities, if not stated otherwise, and represent the second model year of simulations, counting from the restart.

The second section of the chapter presents a comparison of the simulated annual variations of water vapor column density with those observed with SPICAM. The SPICAM data represent an average over 5 Martian years (MY27–31). The model reproduces both the seasonal asymmetry of the hydrological cycle and the total amount of water vapor in the atmosphere. The discrepancies between the observed and simulated quantities do not exceed $\sim$10 pr.μm, and vary with seasons and latitudes.

The seasonal and spatial coverage of the SPICAM data allows for comparing both zonally averaged water cycle and longitude-latitude maps of water vapor column density with MGCM results. The examples of such maps, where SPICAM data were averaged over 5 Martian years, are presented in the **third section of the chapter**. The similar quasi-symmetric (with respect to the north pole) peaks in longitudes may be noticed between $L_s = 90°$ and 150° (see e.g. Figure 2).

In the solar occultation mode, SPICAM IR (1.38 μm-band) channel has conducted measurements of 82 vertical water profiles during MY28. The eclipses

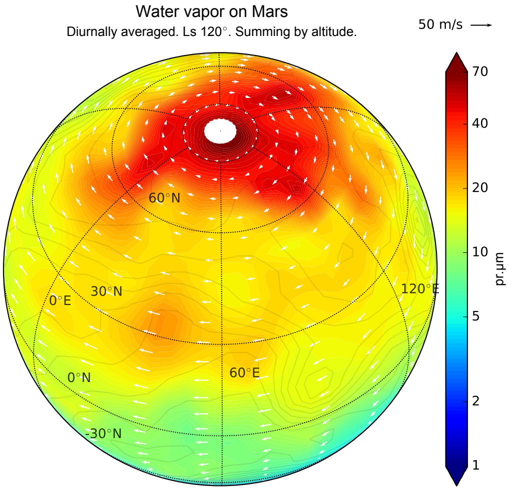

Fig. 2 — Diurnally averaged water vapor column density in precipitable microns (log-scale) in orthographic projection over the season $L_s \sim 120°$ (northern hemisphere summer). Arrows show average horizontal wind velocities in m s^{-1}.

were recorded from $L_s \sim 255°$ to $L_s \sim 300°$, 49 of them in the northern hemisphere and 33 in the southern one. According to the solar occultation technique, each profile corresponds to a specific time and location. We have chosen the interval between $L_s = 255°$ and $L_s = 267°$ for comparison to exclude the period with the major dust storm of MY28. The results for 6 profiles from that period are shown in **the forth section of the chapter**. The comparison is generally favorable, especially for vapor where the Pearson correlation coefficient between the observational and model data does not fall below 0.91. Finally, to complete the comparison with observations, it is required to focus on the ice mixing ratio retrievals. For that, 410 assembled limb-viewing observations from CRISM are used to verify the compliance of the MGCM simulations with the experiment.

Having compared the simulations versus the available observations and verified the ability of the model to reproduce the hydrological cycle, it is possible to turn to a comparison of different model scenarios: three with the mono-modal and one with the bimodal dust particle size distributions. Under the first mono-modal scenario M1, the number of large particles is the same as in the bimodal one, but there are no small particles at all. Thus, the total number of all particles in M1 is less than in the bimodal case. The second mono-modal scenario M2 includes the same total number of particles as the bimodal one, but also without small particles. The third mono-modal scenario M3 is the same as M1, but the microphysical code was turned on only every tenth model time step (every 200 seconds), that is, with a tenfold increase of the microphysical time step. In **the fifth section of the chapter** the simulations under these mono-modal scenarios have been performed similarly to the bimodal one described above.

Simulations for mono-modal and bimodal particle size distributions demonstrated that the latter scenario most strongly affects the modeled ice clouds mass, opacity, number density and particle radii bringing them closer to observations. The simulations showed much weaker effect of the bimodality (excess of small aerosol particles) on water vapor distributions. The use of the second peak of small CCN in the bimodal distribution increases the number of particles nucleated in the atmosphere, which contributes to the growth of ice mass, increases the concentration of ice particles and reduces their radii. This, in turn, improves the simulated opacity of the clouds compared to observations.

More generally, these results highlight the importance of the dust size distribution with the peak of small particles for modeling water ice in the atmosphere of Mars. Also, it is reasonable to expect that these distributions throughout all seasons and locations are not perfectly bimodal, but have more complex shapes. More measurements and MGCM simulations that self-consistently account for dust transport can further clarify this and shed the light on the modality of the dust size distribution.

The forth chapter describes the seasonal water "pump" mechanism: vertical transport of water vapor from the lower and middle atmosphere of Mars to the thermosphere. **The first section of the chapter** presents the design of simulations. The extended (up to 160 km) model version is used in this chapter. As a result, the water vapor photodissociation is included in the hydrological scheme. The model has been initialized with the distribution of water vapor and ice obtained in the basic model version [2]. The latter runs have been performed for several Martian years until the model achieved a quasi-steady state (repetition of distributions with seasons). Since the current version of the MGCM extends higher into the thermosphere, the additional vertical levels have been initialized with the values at ~100 km. The initial conditions for the dynamical fields are taken from the simulations of Medvedev et al. (2016). In this chapter, two predetermined dust scenarios are employed. The "basic" one is the same as in the previous chapter. The second one is based on the measurements for the Martian Year 28 (MY28), which included a major dust storm during the perihelion season .

Vertical transport of water vapor and ice is best characterized by the corresponding fluxes. **The second section of the chapter** presents latitude-seasonal distributions of the vertical water vapor flux at several altitudes simulated using the "basic" dust scenario. It clearly shows that at all altitudes above 30 km, the flux maximizes around perihelion between $L_s = 200°$ and $300°$ and is negligibly small throughout the rest of the year.

The third section of the chapter explores the perihelion season and considers the water transport in more detail. Figure 3a presents the water vapor amount in ppmv averaged diurnally and between $L_s = 250°$ and $270°$. Streamlines show the residual meridional circulation, while their thickness and color indicate the magnitude and vertical direction of the water vapor flux, correspondingly. In agreement with previous observations and simulations, it is seen that the dominant part of water vapor concentrates in the southern (summer) hemisphere below ∼45 km. Water increasingly sublimates near the surface at middle to high latitudes and is transported up- and northward by the meridional cell. This results in the water vapor maximum of up to a few hundred ppmv at around 30 km that extends in latitude to ∼45°N. Water ice clouds (shown with white contours) form immediately above and are transported by the meridional circulation in the same manner as vapor. Color shades in Figure 3a demonstrate an elevated amount of water vapor (∼90–140 ppmv) in the high-latitude "bottleneck" between ∼60 and 90 km. Higher up at around the mesopause and in the lower thermosphere (see Figure 3c), the water vapor is effectively transported across the globe by the meridional circulation, and its magnitude increases up to ∼160 ppmv (in the average sense mentioned above).

The forth section of the chapter reveals the causal relationship between the high-altitude water and atmospheric dust. Figure 3d shows that temperature increased by ∼20 K over the south pole and by more than 30 K over the north pole at 45 km (see color contours for temperature differences with the "basic" dust scenario). The meridional transport intensified during the dust storm. In particular, the warming over the winter pole is caused adiabatically by the downward branch of the circulation cell. The changes in temperature and transport remarkably affected atmospheric water. Another effect of the dust storm captured by the model is the increase of CCN in the atmosphere. A larger number of nuclei aids water vapor condensation, the formed ice particles have smaller radii and, thus, slower sedimentation speed. Therefore, water ice clouds form higher, which too contributes to increased water abundances in the upper atmosphere.

The fifth section of the chapter demonstrates that, for the "basic" dust scenario, the vertical velocity exhibits a mixture of the diurnal and semidiurnal tides with phase advancing with height. The downward phase tilt is the manifestation of the tide generated below and propagating upward. The angle of the tilt progressively changes with altitude above ∼70 km to almost

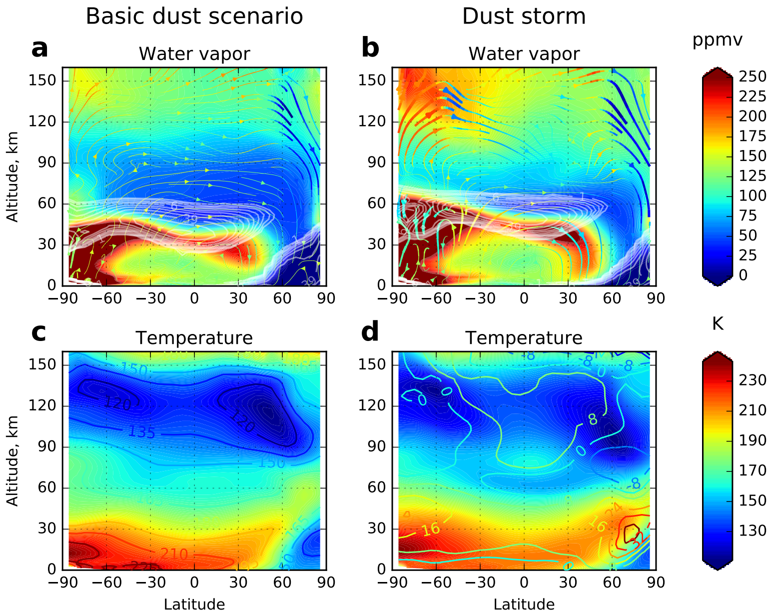

Fig. 3 — Latitude-altitude cross-sections of the quantities simulated for the "basic" dust scenario (left column) and the MY28 dust storm (right column): (a) Water vapor (shaded), water ice (white contours) and the meridional flux of water vapor (the lines with arrows, the color and thickness of which indicate the vertical direction and magnitude, correspondingly); (b) is the same as in panel (a), but for the dust storm of MY28; (c) temperature (shaded) for the "basic" dust scenario; (d) is the same as in (c), but for the MY28 dust storm scenario, except for the contour lines that show the temperature difference between (d) and (c). All fields are averaged zonally and over the period between $L_s = 250°$ and $270°$.

vertical, indicating the increasing role of the in situ-excited tides in the upper atmosphere. Unlike the vertical velocity, water vapor varies mainly with the diurnal periodicity with the maximum magnitude of ~120 ppmv at 30 km. Interactions with the semidiurnally varying vertical velocity form a characteristic steep reversal of water anomalies at 40 km by pushing water up and down twice per day.

In order to validate the simulations, in **the sixth section of the chapter**, they are compared with the data inferred from the measurements by the MCS–MRO during MY28. The authors of the latter study used an indirect method to estimate the water vapor and ice abundances from the observations of temperature and water ice clouds. MCS performs 13 polar orbits per Martian sol. Away from the poles, the groundtrack of MRO corresponds to approximately 15:00 hours local solar time on the ascending side of the orbit and to ∼3:00 local time on the opposite side. Since MCS orbits vary, the model output is averaged over the intervals 14:00–16:00 and 2:00–4:00 hours local time for comparison, correspondingly. Both observations and modeling show gradual, but rapid increase of the total water abundance and its rise in altitude towards the perihelion season.

The main findings described in this section are the following:

– Water is lifted up in high latitudes of the summer hemisphere by the upward branch of the pole-to-pole meridional circulation cell. Then water vapor is transported by the latter across latitudes in the mesosphere and thermosphere.
– Water can penetrate upper levels only during the perihelion season, when the meridional circulation cell is sufficiently strong.
– The influx of water into the middle and upper atmosphere increases, whenever the meridional cell intensifies, for instance, during dust storms. In addition, dust storm-induced heating increases the amount of water vapor in the lower atmosphere.
– Upward transport of water is significantly modulated by the solar tide. The latter acts as a "pump" by increasing the transport during certain local times and almost completely shutting it down during the others.

In **conclusion**, the main results of the thesis are given. The main results of the thesis coincide with the provisions submitted to defense.

Author’s publications on the dissertation topic

1. *Shaposhnikov, D. S.* The water cycle in the general circulation model of the martian atmosphere / D. S. Shaposhnikov, A. V. Rodin, A. S. Medvedev // Solar System Research. — 2016. — Vol. 50, no. 2. — P. 90—101.
2. Modeling the hydrological cycle in the atmosphere of Mars: Influence of a bimodal size distribution of aerosol nucleation particles / D. S. Shaposhnikov [et al.] // Journal of Geophysical Research: Planets. — 2018. — Vol. 123, no. 2. — P. 508—526.
3. Seasonal Water “Pump” in the Atmosphere of Mars: Vertical Transport to the Thermosphere / D. S. Shaposhnikov [et al.] // Geophysical Research Letters. — 2019. — Vol. 46. — P. 4161—4169.
4. *Shaposhnikov, D. S.* Fazovye prevrashhenija i obmen vody mezhdu atmosferoj i poverhnost’ju v chislennoj modeli obshhej cirkuljacii atmosfery Marsa [Phase transformations and water exchange between the atmosphere and the surface in the general circulation numerical model of the Martian atmosphere] / D. S. Shaposhnikov, A. V. Rodin // Problemy sovremennoj fiziki. Trudy 57-j nauchnoj konferencii MFTI [Problems of modern physics. Proceedings of the 57th Scientific Conference of MIPT]. — 2014. — P. 197—198.
5. *Shaposhnikov, D. S.* Diffuzija passivnoj primesi v gidrologicheskom cikle modeli obshhej cirkuljacii atmosfery Marsa MAOAM [Diffusion of a passive tracer in the hydrological cycle of the Martian general atmosphere circulation model MAOAM] / D. S. Shaposhnikov, A. V. Rodin, A. S. Medvedev // Sovremennye problemy distancionnogo zondirovanija Zemli iz kosmosa [Modern problems of remote sensing of the Earth from space]. — 2016. — P. 223—223.

6. *Shaposhnikov*, *D. S.* Gidrologicheskij cikl v chislennoj modeli obshhej cirkuljacii atmosfery Marsa [Hydrological cycle in the general circulation numerical model of the Marian atmosphere] / D. S. Shaposhnikov, A. V. Rodin, A. S. Medvedev // Problemy sovremennoj fiziki. Trudy 59-j nauchnoj konferencii MFTI [Problems of modern physics. Proceedings of the 59th Scientific Conference of MIPT]. — 2016. — P. 37—38.

7. *Shaposhnikov*, *D. S.* Blok gidrologicheskogo cikla v chislennoy modeli global'noy cirkuljacii atmosfery Marsa [The hydrological cycle block in the numerical model of the global circulation of the atmosphere of Mars] // Certificate of state registration of computer programs № 2019611779 (date of registration 04.02.2019) / D. S. Shaposhnikov. — 2019.

Shaposhnikov Dmitry Sergeevich

Numerical Simulation of the Hydrological Cycle of Mars

Автореф. дис. на соискание ученой степени к.ф.-м.н.

Подписано в печать ___.___._____. Заказ № ____________

Формат 60×90/16. Усл. печ. л. 1. Тираж 20 экз.

Типография ____________________________________